

Flux-line interactions with precipitates in $\text{YBa}_2\text{Cu}_3\text{O}_{7-x}$ films revealed by scanning Hall probe microscopy

A. N. Grigorenko and S. J. Bending

Department of Physics, University of Bath, Bath BA2 7AY, United Kingdom

G. D. Howells

Oxford Instruments, Research Instruments, Tubney Woods, Abingdon OX1 5QX, United Kingdom

R. G. Humphreys

DERA, St. Andrew's Road, Malvern, Worcestershire WR14 3PS, United Kingdom

(Received 30 September 1999; revised manuscript received 11 February 2000)

We have used scanning Hall probe microscopy to study the interaction between flux lines and a random array of precipitates in thin YBCO films. Pinning by precipitates has been demonstrated by measuring the distribution and magnetic field profiles of individual flux lines. Flux lines in the film with precipitates have strongly preferred locations as well as a much broader range of shapes and sizes compared to YBCO films without precipitates. We have also observed “local magnetization” anomalies, which appear at multiples of the matching field for the random array of pinning sites.

I. INTRODUCTION

Vortex interactions with pinning sites in type-II superconductors have attracted renewed interest since the discovery of high- T_c materials. Flux pinning is key in many important superconductor applications as well as giving rise to rich magnetization and critical current phenomena.¹⁻³ Recently attention has focused on investigations of flux pinning in regular (periodic) arrays of artificial pinning sites.⁴⁻⁸ This interest arises from the fact that arrays of pinning centers can stabilize ordered vortex configurations leading to striking anomalies in the magnetization⁶⁻⁸ and the critical current.^{5,9} The existence of these anomalies is attributed to commensurability effects and has been extensively studied both experimentally⁶⁻¹⁰ and theoretically.¹⁰⁻¹²

Since most natural type-II superconducting materials contain randomly distributed pinning sites it is worthwhile investigating vortex interactions with controlled irregular (random) arrays of pinning centers (e.g., columnar defects) to gain better insight into their properties. Commensurability effects should also be important in this case, where a “Mott insulator” phase was predicted for the flux line system¹³ at the matching field when the number of flux lines equals the number of pinning sites. Many experiments have been performed with random pinning sites, but nearly all were focused on the measurement of some average superconductor parameters, e.g., bulk magnetization or critical current. In this paper we present a systematic study of flux line interactions with a random array of pinning sites in thin YBCO films performed by scanning Hall probe microscopy (SHPM).¹⁴ In contrast to many other techniques, SHPM can resolve individual vortices with high spatial and magnetic field resolution as well as fair temporal resolution.¹⁵⁻¹⁷ This has allowed us to map the magnetic field produced by discrete flux lines and observe their dynamics at temperatures very close to T_c with $t = 1 - T/T_c > 0.005$.

Two main topics have been covered by our investigation.

First, we have imaged static field-cooled flux structures in a thin superconducting film with precipitates and demonstrated that the flux lines are preferentially pinned at precipitates. Secondly, we have studied the flux line dynamics upon sweeping the applied magnetic field close to T_c . For the first time we have resolved weak matching anomalies in the “local magnetization” produced by flux lines in a thin YBCO film with a low density random array of strong pinning sites. The paper is constructed as follows. Section II describes the experimental apparatus and the samples. Section III deals with static field-cooled measurements of flux structures in thin YBCO films with precipitates and a comparison with those in stoichiometric films. In Sec. IV we describe the anomalies for the random array of pinning sites resolved in the “local magnetization” loops close to T_c . Finally, some conclusions are drawn.

II. EXPERIMENTAL APPARATUS AND SAMPLE PREPARATION

The design of the scanning Hall probe microscope has been described in detail elsewhere.¹⁴ In brief, it is based upon a custom-built low-temperature scanning tunnelling microscope (STM) where a microfabricated semiconductor chip replaces the usual STM tip. This can then be used to measure the distribution of the normal component of magnetic field and/or the surface topography. The sensor is patterned in a GaAs/AlGaAs heterostructure two-dimensional electron gas and consists of a $0.85 \mu\text{m}$ Hall probe and an etched mesa coated with a thin layer of gold which acts as an integrated STM tip. The sample is tilted 1° – 2° with respect to the Hall probe to ensure that the STM tip is always the closest point to it and brought into tunnelling contact with an inertial approach mechanism. The experiments were performed in a “flying” mode whereby the STM tip is used to find the surface after which the sample is retracted a distance of about $\sim 0.5 \mu\text{m}$ from the Hall probe in order to perform

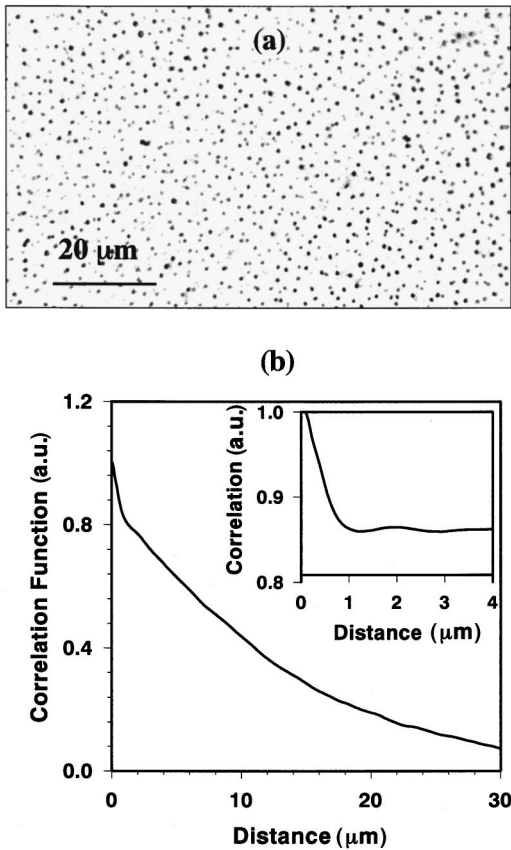


FIG. 1. (a) Optical micrograph of a YBCO thin film with precipitates and (b) correlation function of the precipitate distribution. Inset shows correlation function after subtraction of a linear background.

very rapid magnetic imaging without STM feedback.

The YBCO film was grown on an MgO substrate at 690 °C by electron beam coevaporation of the metals in the presence of atomic oxygen with a subsequent anneal, also in atomic oxygen.¹⁸ (Note that annealing in atomic oxygen usually results in overdoping.) The sample was deliberately grown with excess Cu to produce a low density random array of Cu rich precipitates. Several stoichiometric YBCO films with the same thickness were grown under the same conditions and contained no precipitates and these have been used as reference samples ($T_c = 90.8$ K by magnetization). The (001) Cu-rich film studied here was 0.35 μm thick and had a critical temperature of 86.4 K as measured by magnetization with a 10^3 A cm^{-2} persistent current density detection criterion. This temperature corresponds to the very foot of the resistive transition. The precipitates consisted of a nonsuperconducting phase, had sizes in the range of 0.2–2 μm , and were homogeneously distributed in the film with a density of about $2.5 \times 10^7 \text{ cm}^{-2}$ yielding a mean matching field of ~ 5 G. Figure 1(a) shows a typical optical micrograph of the surface of the film with precipitates and Fig. 1(b) plots the correlation function $C(R) = \langle \rho(r+R)\rho(r) \rangle$ of the precipitate density calculated from the digitised micrograph. When the separation R is smaller than the precipitate size, the precipitates overlap with themselves producing the initial peak in the correlation function. From this structure we estimate a mean precipitate size of $\sim 0.8 \mu\text{m}$. Beyond this peak the

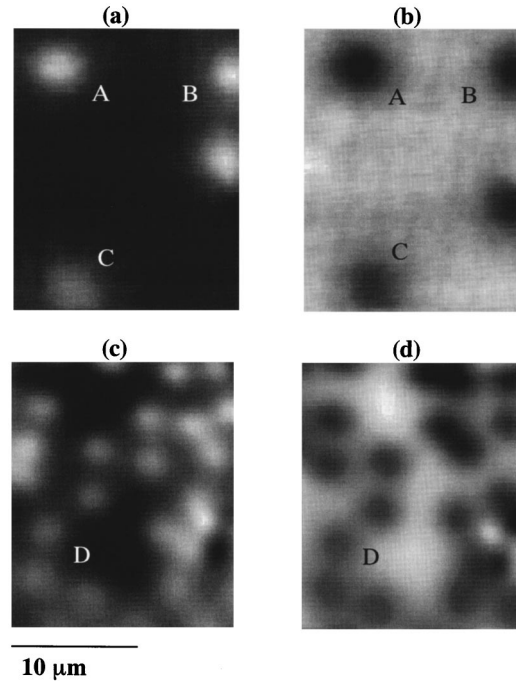


FIG. 2. SHPM images of a YBCO thin film with precipitates after field cooling to 77 K in (a) 0.1 Oe (gray scale spans 0.73 G), (b) -0.1 Oe (gray scale spans 0.8 G), (c) 1.1 Oe (gray scale spans 1.1 G), (d) -0.9 Oe (gray scale spans 1.1 G).

correlation function shows an approximately linear decay with a weak modulation superimposed upon it. The latter is more clearly seen in the inset of Fig. 1(b), where the linear component of $C(R)$ has been subtracted, and yields an average first nearest-neighbor distance of $\sim 2.0 \pm 0.5 \mu\text{m}$. We note that the distribution of the precipitates is not even approximately periodic at any important length scales [see Fig. 1(a)]. It is, however, *regular* in the sense that the precipitate density and the distance between first nearest neighbors is fairly constant over the whole $4 \text{ mm} \times 7 \text{ mm}$ sample.

III. STATIC FIELD-COOLED FLUX CONFIGURATIONS IN YBCO FILMS WITH PRECIPITATES

Since the precipitates in the YBCO films studied were nonsuperconducting they should represent effective pinning sites for flux lines. Unfortunately, due to very poor quality tunnelling, we were unable to simultaneously image a precipitate and a flux line pinned on it. However, the following sets of observations confirm, beyond reasonable doubt, the preferential pinning of flux lines at precipitates.

We find that flux lines of opposite polarities tend to be located at the same positions in the scanning area of the sample for field-cooled images with the reversed direction of magnetic field (see the vortices A, B, C, and a cluster of vortices D in Fig. 2). In all field-cooled images at low fields, flux lines tended to occupy the same locations in the sample for repeated cooling cycles at the same applied magnetic field. While this behavior is not particularly surprising, it differs markedly from that of stoichiometric YBCO films without precipitates, where the flux lines frequently occupy new positions after different cooling cycles in the same magnetic field.

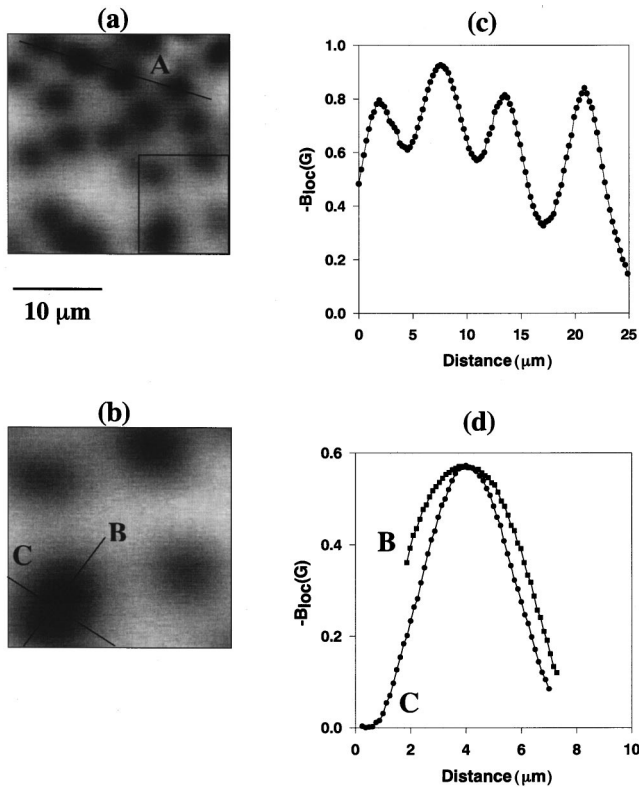


FIG. 3. SHPM images of a YBCO thin film with precipitates after field cooling to 77 K in (a) -0.52 Oe (gray scale spans 0.8 G). (b) Close up of the part of image (a) enclosed in the box. Line scans with inverted contrast (c) along line A of image (a), and (d) along lines B and C of image (b).

Line scans across the vortex images, Figs. 3 and 4, reveal that the flux lines have a much broader range of shapes and sizes than those in YBCO films without precipitates (see Figs. 2 and 3 in Ref. 19). In addition, line scans sometimes reveal an unusual internal structure to a vortex as illustrated in Fig. 3(c). In previous work a model of the response of a Hall probe to a local region of magnetic flux much smaller than the size of the Hall probe was developed.²⁰ This response function is a bell-shaped curve of width approximately equal to the size of the Hall probe. When a flux line is pinned by a precipitate with a size comparable to the width of the response function, the measured Hall voltage shows a pronounced peak when the two objects exactly coincide. Figure 3(c) shows a linescan over four adjacent vortices and this peaklike structure can be clearly seen on the first and the last flux line of the row implying that the dimensions of these two precipitates were close to those of the Hall probe. Despite having different core sizes, the field profiles appear to have a universal decay length at a given temperature, supporting the picture of flux lines pinned on precipitates. Figures 3(b) and 3(d) show an expanded view of a structure at the bottom of the scanning area. Judging by the way this feature develops with increasing field we believe it represents two flux lines very close together, although we are unable to resolve them individually. At this separation flux line repulsion must be very strong indicating that both are firmly pinned on adjacent precipitates (see later estimates).

Finally, upon decreasing the temperature the measured flux line half widths show a tendency to saturate towards a

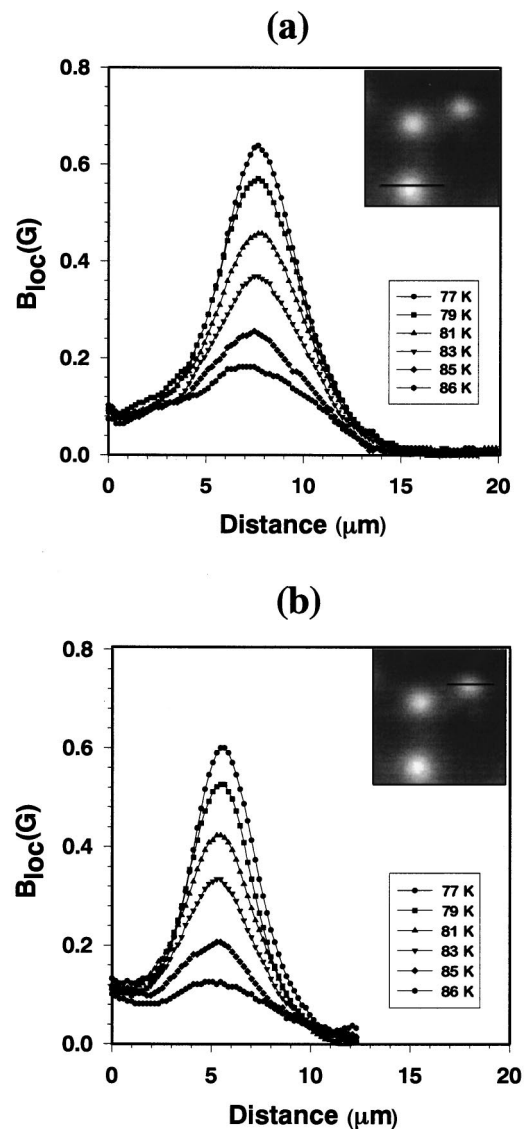


FIG. 4. Line scans along the flux line (a) at the bottom of the SHPM image of a YBCO thin film with precipitates shown in the inset, and (b) at the top of the image at different temperatures.

size which is much larger than vortex diameters in precipitate-free YBCO films at the same temperature, as well as being larger than the dimensions of the Hall probe. Figure 4 depicts the temperature dependencies of line scans for two different flux lines with a saturation diameter of ~ 5 μm [Fig. 4(a)] and ~ 3 μm [Fig. 4(b)] respectively. Typical vortex diameters for stoichiometric YBCO films without precipitates were ~ 2 μm at 77 K,¹⁶ which is considerably smaller than our measured values. For vortices in precipitate-free YBCO films we cannot rule out the possibility that our flux profiles are broadened due to thermal fluctuations of the core position which may sample several adjacent pinning sites. Such fluctuations are known to be strong quite far from T_c in very anisotropic materials such as $\text{Bi}_2\text{Sr}_2\text{CaCu}_2\text{O}_{8+\delta}$, but in strongly pinning YBCO thin films with modest anisotropy are only expected to become important rather close to T_c . We note that we were only able to image vortices up to $t = 0.95$ in stoichiometric films while they are quite well resolved up to $t = 0.995$ in our measurements on Cu-rich films.

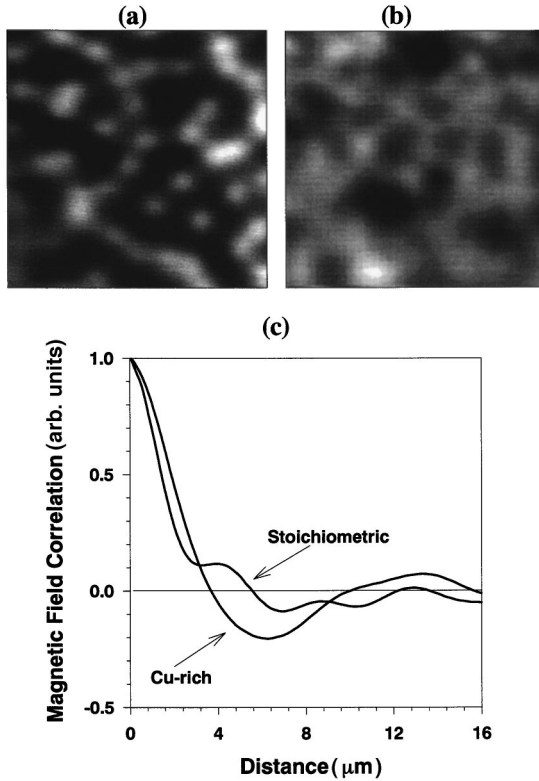


FIG. 5. SHPM images of (a) a YBCO film without precipitates after field-cooling to 77 K in 2 Oe (gray scale spans 1.1 G) (b) a YBCO film with precipitates after field cooling to 77 K in 2 Oe (gray scale spans 2.2 G). (c) Correlation functions of magnetic induction deduced from the magnetic field distributions shown in Figs. 5(a) and 5(b).

This may well be a consequence of thermal fluctuations in the former and is further indirect evidence that flux lines are strongly pinned on precipitates until very close to T_c .

Taken together, all these observations demonstrate that flux lines are preferentially pinned by precipitates and yield an estimate of the mean precipitate size of the order of the Hall Bar size $\sim 0.85 \mu\text{m}$, which is close to the value obtained from the precipitate correlation function. Assuming all flux lines to be pinned on precipitates at low fields, their separation distribution in the field-cooled images allows one to evaluate the pinning force. A lower bound can be placed on this by considering the two very close flux lines (spacing $\sim 1 \mu\text{m}$) shown in Fig. 3(b). As was recently pointed out in Ref. 21 the crystalline anisotropy of YBCO places our $0.35 \mu\text{m}$ films in the “thin” limit when the force between two flux lines separated by a distance r ($r \ll 2\lambda^2/d$) is given by²²

$$f = \frac{\Phi_0^2 d}{8\pi^2 \lambda^2 r}, \quad (1)$$

where Φ_0 is the flux quantum, λ is the bulk penetration length and d is the film thickness. This yields a lower bound estimate of the pinning force of about $\sim 10^{-7}$ dyne at 77 K ($t=0.89$). It is interesting to compare pinning in Cu-rich YBCO films to that in those without precipitates. Figure 5 shows magnetic field distributions and correlation functions [constructed as for Fig. 1(b)] for a reference stoichiometric YBCO film and the sample with precipitates after field cool-

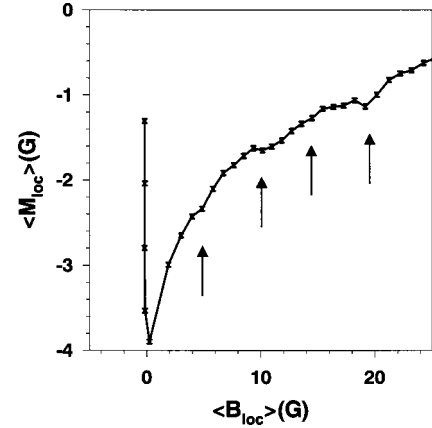


FIG. 6. The “local magnetization” averaged over the scanning area as a function of the mean local induction at 86 K extracted from the initial part of the hysteresis loop after zero field cooling.

ing to 77 K in 2 Oe. At this field individual vortices cannot be clearly resolved and pinning manifests itself in the form of pronounced fluctuations in the local magnetic induction. The gray scale of the precipitate sample is twice as large as the stoichiometric film indicating that a stronger pinning force which can sustain larger flux gradients is at work. In addition the correlation function of the Cu-rich sample has a much broader distribution and the peak near $\sim 4 \mu\text{m}$ corresponding to short-range flux line ordering is absent.

It is also interesting to note that the interaction between flux lines is clearly repulsive at small applied fields (low flux line densities) when they tend to be homogeneously distributed [see Figs. 2 and 3(a)]. At higher fields, however, we observe a tendency for chain formation [Fig. 3(a)]. It is well known that relatively large artificial pinning centers can stabilize multiquanta vortices²³ when two or more flux lines are trapped on one pinning center. However, these multiquanta states should only be observed at high magnetic fields when the distance between flux lines is small, and experimentally it is almost impossible for us to distinguish between a double flux quantum and two closely spaced single flux quanta.

IV. MATCHING ANOMALIES FOR THE RANDOM ARRAY OF PINNING CENTERS

An important advantage of the scanning Hall probe microscope is its very high magnetic field resolution ($\sim 30 \text{ nT}/\sqrt{\text{Hz}}$ at 77 K) which allows the resolution of flux lines and the measurement of their dynamics in the film under study at temperatures up to 86 K, which is very close to $T_c = 86.4 \text{ K}$. We have studied “local magnetization” M_{loc} (as defined by $M_{loc} = B_{loc} - H_{appl}$, where H_{appl} is the applied field and B_{loc} is the local induction) loops for the YBCO film with precipitates at various temperatures. A typical scanning region of $25 \times 25 \mu\text{m}^2$ was very much smaller than the sample size yet still contained a large number (>100) of precipitates. Thus, the average of the “local magnetization” over the 128×128 pixels in the scan area yields the mean local response of a reasonably large ensemble of precipitates. $\langle M_{loc} \rangle$ extracted from major hysteresis loops showed a characteristic cusp¹⁰ close to the matching field of about 5 Oe at temperatures close to the transition temperature.

These weak anomalies were, in fact, observed more

clearly in $\langle M_{\text{loc}} \rangle$ extracted from the initial parts of hysteresis loops after zero field cooling. Figure 6 shows this quantity as a function of the mean local induction at 86 K. Four weak anomalies (plateaux and minima) can be seen at approximately equal intervals of $B_m = 5$ G, which are significantly larger than the noise level indicated by the error bars. The plateaux and minima shown in Fig. 6 became more pronounced for temperatures closer to the transition temperature and disappeared completely below 83 K.

We note that these measurements were performed at temperatures very close to T_c when the pinning force is small and the flux mobility is high. Consequently, the anomalies in $\langle M_{\text{loc}} \rangle$ may occur when the local density of flux lines matches the local density of precipitate pinning centres. The matching field B_m is in this case

$$B_m = n_{\text{loc}} \Phi_0, \quad (2)$$

where n_{loc} is the local density of pinning centres and Φ_0 is the flux quantum. We stress that Eq. (2) describes the local matching condition. The matching field will be different for regions of the sample with different precipitate densities and matching anomalies will only appear in the bulk magnetization if fluctuations of the density of pinning centers are small or there are comparatively large regions with a constant density. Using Eq. (2) we estimate the local density of precipitates as $n_{\text{loc}} = \Phi_0 / B_m = 2.5 \times 10^7 \text{ cm}^{-2}$ which is in a good agreement with the precipitate density obtained from optical micrographs.

V. CONCLUSION

In conclusion, we present a range of measurements which demonstrate that the precipitates formed naturally in Cu-rich YBCO films represent preferential pinning sites for flux lines. The latter repel each other at low densities but appear to show some tendency for chain formation at higher densities. A comparison between Cu-rich and stoichiometric YBCO films confirms these conclusions. Weak anomalies were observed in the average ‘‘local magnetization’’ for the Cu-rich samples during magnetic field cycling. In particular up to four orders of peaks were seen at approximately equal intervals in the initial part of zero-field-cooled hysteresis loops as a function of the mean local induction very close to T_c . We suggest that these anomalies occur when the local density of flux lines matches the local density of the pinning centers. The results of our study imply that the deliberate inclusion of precipitates could be used to increase the critical current of thin films and suppress flux noise in superconducting devices.

ACKNOWLEDGMENTS

This work was jointly supported EPSRC and UK MOD by EPSRC Grant No. GR/L96448.

-
- ¹C. P. Bean and J. D. Livingston, Phys. Rev. Lett. **12**, 14 (1964).
²G. Blatter *et al.*, Rev. Mod. Phys. **66**, 1125 (1994).
³E. H. Brandt, Rep. Prog. Phys. **58**, 1465 (1995).
⁴A. F. Hebard, A. T. Fiory, and S. Somekh, IEEE Trans. Magn. **1**, 589 (1977).
⁵A. N. Lykov, Solid State Commun. **91**, 531 (1993).
⁶M. Baert, V. V. Metlushko, R. Jonckreere, V. V. Moschalkov, and Y. Bruynseraede, Europhys. Lett. **29**, 157 (1995).
⁷M. Baert, V. V. Metlushko, R. Jonckreere, V. V. Moshchalkov, and Y. Bruynseraede, Phys. Rev. Lett. **74**, 3269 (1995).
⁸K. Harada *et al.*, Science **274**, 1167 (1996).
⁹D. J. Morgan and J. B. Ketterson, Phys. Rev. Lett. **80**, 3614 (1998).
¹⁰V. V. Moshchalkov *et al.*, Phys. Rev. B **54**, 7385 (1996).
¹¹L. D. Cooley and A. M. Grishin, Phys. Rev. Lett. **74**, 2788 (1995).
¹²C. Reichhardt, J. Groth, C. J. Olson, S. B. Field, and F. Nori, Phys. Rev. B **54**, 16 108 (1996).
¹³D. R. Nelson and V. M. Vinokur, Phys. Rev. B **48**, 13 060 (1993).
¹⁴A. Oral, S. J. Bending, and M. Henini, Appl. Phys. Lett. **69**, 1324 (1996).
¹⁵A. M. Chang *et al.*, Appl. Phys. Lett. **61**, 1974 (1992).
¹⁶D. Davidovich *et al.*, Phys. Rev. Lett. **76**, 815 (1996).
¹⁷S. Field, J. Siegel, and J. Witt (unpublished).
¹⁸N. G. Chew, IEEE Trans. Appl. Supercond. **5**, 1167 (1995).
¹⁹A. Oral, S. J. Bending, R. G. Humphreys, and M. Henini, Supercond. Sci. Technol. **10**, 17 (1997).
²⁰S. J. Bending and A. Oral, J. Appl. Phys. **81**, 3721 (1997).
²¹A. V. Kuznetsov, D. V. Eremenko, and V. N. Trofimov, Phys. Rev. B **59**, 1507 (1999).
²²J. Pearl, in *Low Temperature Physics-LT9*, edited by J. G. Daunt, D. O. Edwards, F. J. Milford, and M. Yaqub (Plenum, New York, 1965), Pt. A, p. 566; Appl. Phys. Lett. **5**, 65 (1964).
²³G. S. Mkrtchyan and V. V. Schmidt, Zh. Eksp. Teor. Fiz. **61**, 367 (1971) [Sov. Phys. JETP **34**, 195 (1972)].